VINE PLOT DETECTION IN AERIAL IMAGES USING FOURIER ANALYSIS

C. Delenne*, G. Rabatel, V. Agurto**, M. Deshayes***

*UMR TETIS - Maison de la Télédétection - 500 rue JF Breton, 34093 Montpellier
**UMR ITAP - CEMAGREF - 361 rue JF Breton, 34196 Montpellier

KEY WORDS: segmentation, remote-sensing, frequency analysis, Gabor filters, vineyard

ABSTRACT:

Vine-plot mapping and monitoring are crucial issues in land management, particularly for areas where vineyards are dominant, like in some French regions. In this context, the availability of an automatic tool for vineyard detection and characterization would be very useful. Due to the periodic patterns induced by this culture, frequency analysis appears to be a very suited tool for vineyard detection in aerial images. A recursive process using Fast Fourier Transform algorithm has been developed to meet this need. This results in vine plot segmentation, with contours in polygonal form and characterization with accurate estimation of interrow width and row orientation. To foster large-scale applications, tests and validation have been carried out on standard very high spatial resolution remote-sensing data. More than 71% of adults, mechanically trained vines have been well detected with 44% having a good contour extraction and 27% beeing grouped by two or three.

1 INTRODUCTION

The considerable increase in digital technologies makes it possible to automatically analyze images, but also to understand them by providing high-level information on their content. Concurrently, a such considerable increase is observed in the availability of very high spatial resolution (VHSR) remote-sensing data. This offers a lot of new potential applications: the shape or the spatial structure of observed objects is becoming more distinguishable, providing greater possibilities for discrimination and characterization, notably in the agricultural domain. Various type of vegetation can thus be distinguished according to their spatial patterns (cereal crops, forests, orchards ...). In this context, automatic analysis methods could be developed to build or update geographical databases for land management.

However, because they deal with spatial structures or shape, these new applications also require new image processing methods. Several shape-model based approaches can thus be found in the literature, especially for building detection (Garcin et al., 2001) (Segl et al., 2003) or isolated trees detection (Barbezat et al., 1996). For forest identification, various textural approaches based on co-occurrence matrices are proposed such as (Franklin et al., 2000) or (Moskal, 2002).

Accurate digital mapping of vineyards for wine-growing regions such as Languedoc-Roussillon (France) could be extremely useful for many reasons. These maps can be integrated within Geographical Information Systems (GIS) which can be used by winegrower cooperatives to improve the monitoring of quality compliance in areas registered in the list of Controlled Origin Denomination. The management of pollution, erosion and flood risks is another field that can take advantage of these maps. Indeed, these risks, depending on culture and soil surface condition, are worsened by mechanization and intensive cropping practices (Wassenaar et al., 2005). User demand usually concerns 1) locating vine plots and 2) identifying some characteristics that can be connected to cropping practices or crop quality (interrow width, orientation of rows, presence of grass between rows ...).

Most vineyard related studies using remote sensing data meet the second requirement by detecting vine rows (Bobillet et al., 2003), or by characterizing training mode (Wassenaar et al., 2002) or foliar density (Hall et al., 2003) for previously delimited plots. They emphasize the relevance of textural analysis applied to submetric spatial resolution images. Indeed, according to the Shannon-Nyquist theorem, periodic patterns resulting from the spatial arrangement of vine plants (often in lines or grid), become perceptible with a spatial resolution that is at least twice as small as the pattern period. In many wine-growing regions, the minimum distance between two vine rows, can be as small as 1 m; consequently, image spatial resolution should be lower than 0.5 m. Because of this periodic organization, a vine pattern can roughly be assimilated to a local planar wave of a given spatial frequency and orientation. Therefore, frequency analysis appears as a suitable approach for vine detection.

Wavelet analysis presented in (Ranchin et al., 2001) is applied to 25 cm resolution images for vine/non-vine pixel classification. Using a plot basis validation, 78 % of plots were accurately classified; but this approach is complex and needs significant user intervention. A Fourier Transform based analysis should be more straightforward and quite as effective since this tool is perfectly suited for oriented and periodic texture detection. Basically, the Fourier spectrum of a vine plot image contains two or four main amplitude peaks, the position of which being directly related to vine row orientation and interrow width. Wassenaar (Wassenaar et al., 2002) successfully used it for vine/non-vine classification and characterization on 25 cm resolution images. This method also gave a very precise estimation of interrow width and row orientation. In (Chanussot et al., 2005), a Radon transform is applied to the Fourier spectrum of a 2 cm resolution image which allows a more precise evaluation of row orientation, used in a further algorithm of missing trees detection.

However, in the examples above, a preliminary delineation of the vine plots is required. We thus address the problem of vineyard detection, segmentation and characterization in VHSR aerial images, without any parcel plan availability. An original recursive scheme is proposed to meet this need. The idea is to isolate each individual plot by selecting the corresponding frequencies in the Fourier spectrum, using a specific Gabor filter. To foster large-scale applications, this process has been applied to standard VHSR aerial images. In the following part, the theoretical aspects of the method are presented, as well as its recursive implementation. Then, results obtained on a 200 ha study area, presenting a large set of vineyard types and conditions, are given and discussed.

2 STUDY AREA AND DATA

Figure 1: Zoom on the study area and the manual segmentation.

In the study area, like in most of vine-growing regions, two main patterns can be observed on aerial images according to vine training mode:

- Grid pattern: about a quarter of the vineyards considered in this study is trained in 'goblet'. This old method of vine training involves no wire or other system of support: vine stocks are planted according to a grid pattern, often square, with approximately 1.5 m $\times$ 1.5 m spacing in the study area but sometime up to 3 m spacing in dry regions.

- Line pattern: most of the recent vineyards are trained using horizontal wires to which the fruiting shoots are tied. Spacing separating two wires is higher than spacing between vine stocks guided by the same wire (often 1 m $\times$ 2.5 m spacing in the study area), which leads to row patterns. More adapted to mechanization, this training mode named trellis, is mainly used.

For tests and validation, data acquisition was made on a 200 ha study area (see figure 1), during the first week of July 2005, when foliar development was such that both vine and soil were visible on aerial images.

Photographs in natural colors (Red, Green and Blue) were acquired by the 'Avion jaune' company using a digital camera aboard an Ultra Light Motorized (U.L.M.). They were geometrically corrected, mosaicked and resampled for a 50 cm resolution. However, the original image required for FFT computation must be in gray levels and, although the three channels have been tested, only the red one is used thereafter, since it provides higher contrast between vine and soil even covered by grass.

Ground-truth information was collected at the same time as image acquisition, especially concerning land use and vine pattern (grid or line). Interrow width (pattern period) and orientation were obtained by precise on-screen measurements.

3 SELECTED APPROACH

The main idea is to isolate each individual plot by selecting the corresponding frequencies in the Fourier spectrum, using a specific Gabor filter.

3.1 Fourier Transform of a vine plot image

Fourier theory states that almost any signal, including images, can be expressed as a sum of sinusoidal waves oscillating at different frequencies. The Fourier Transform amplitude (or Fourier spectrum) of an image I, can be represented in the frequency domain as another image FI. In the conventional representation, this image is symmetric with respect to its center, which contains the average of I, *i.e.* the amplitude of the null frequency F_0. Each position of pixel corresponds to a particular spatial frequency f increasing the further it is from center from $f = 0$ to $f = \pm 0.5$. Its value codes the amplitude of Fourier spectrum, which depends on the presence of the corresponding frequency in the original image I.

Since vineyard patterns on aerial images are periodical and oriented, they induce very located peaks of amplitude in Fourier spectrum (see figure 2).

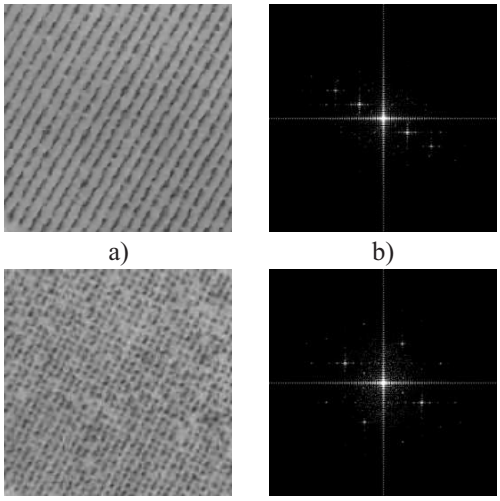

Figure 2: Fourier Transforms of vineyard images. a) row pattern of a treillis vine and b) its Fourier transform on which can be seen two high peaks symmetric with respect to the center. c) Grid pattern of a goblet vine and d) its Fourier transform on which four peaks are present at 90°.

Three characteristics can be deduced from the value and positions of these peaks:

1. peak value can be seen as an estimation of the vine presence in the original image.

2. The angle formed by vector *(center, peak)* with the horizontal line, determines the wave direction in a polar coordinate system, which is perpendicular to the pattern direction *i.e.* the vine row orientation θ.

3. The distance r between one peak and the center, is the frequency f of the corresponding wave ($f \in [0, 0.5]$). This value is directly linked to the pattern period T in pixel *i.e.* the vine interrow width, by $f = 1/T$.

The horizontal and vertical lines intersecting at the spectrum center are due to the non-periodicity of the original image: they represent the frequency components of the image edge discontinuities. These edge-effect peaks, which could mask plot peak detection, can be avoided by applying a Hanning window to the original image before Fourier transform computation (see figure 3). Note that, due to the gray-level attenuation, the modified image is used only for peak detection, the original one being taken again for the filtering process itself.

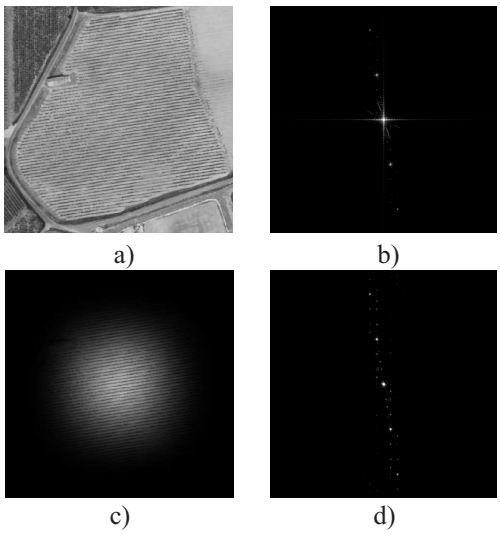

Figure 3: Hanning window effect: a) original image, b) FFT calculation without Hanning window, c) original image multiplied by the Hanning window, d) FFT calculation with Hanning window.

3.2 Gabor Filters

Gabor filters, introduced by Dennis Gabor in the forties (Gabor, 1946), have been widely used, both as a fundamental wavelet decomposition function, and for texture segmentation (Jain and Farrokhnia, 1991), (Weldon et al., 1996).

In the spatial domain, a Gabor filter is defined by an impulse response, which is a complex sinusoid with frequency (u_0, v_0), modulated by a Gaussian envelop $g(x, y)$:

$$h(x, y) = g(x, y) \cdot e^{-2\pi j(u_0 x + v_0 y)} \tag{1}$$

where :

$$g(x, y) = \frac{1}{2\pi\sigma^2} \cdot e^{-\frac{x^2+y^2}{2\sigma^2}} \tag{2}$$

In the frequency domain, the Fourier transform of $h(x, y)$ is a Gaussian function (Fourier transform of $g(x, y)$) centered on the frequency (u_0, v_0):

$$FT\,(h(x, y)) = H(u, v) = G(u - u_0, v - v_0) \tag{3}$$

where:

$$G(u, v) = e^{-2\pi^2\sigma^2(u^2+v^2)} \tag{4}$$

Therefore, the Gabor filter acts as a Gaussian band-pass filter, which can be used to select a given range of frequencies around a particular amplitude peak centered on (u_0, v_0) in the Fourier spectrum. The parameter σ is the filter width. A large value of σ will decrease the accuracy of plot edge location while a too small value, which corresponds to a large filter radius in the spectral domain, will decrease the filter selectivity. A value of about eight pixels, leading to a filter support width of about 2% of the total frequency range in the spectral domain, appears to be a good trade-off. It corresponds to a plot edge location inaccuracy of a few meters.

The filtering process can be applied directly in the Fourier domain:

$$TF\,(O(u, v)) = TF\,(I(u, v)) \cdot H(u, v) \tag{5}$$

where $TF\,(I(u, v))$ is the Fourier transform of $I(x, y)$.

The final result image $O(x, y)$ is then obtained as the inverse Fourier transform of $TF\,(O(u, v))$.

Because the filter function $H(u, v)$ is not symmetric, the resulting image O(x,y) has complex pixel values (only one amplitude peak in the original Fourier spectrum is preserved, instead of the two symmetric ones issued from the real image $I(x, y)$). This property is useful in the present case: by simply computing the modulus of the complex image $O(x, y)$, we directly obtain the amplitude of the selected sinusoidal waves. By comparison, a real output image with real sinusoidal undulations (issued from a symmetric filtering) would have required a supplementary crest detection step to achieve vineyard plot segmentation. In a last step, the modulus image is subject to a binary thresholding to separate vine plots from background.

Figure 4 shows two examples of Gabor filtered outputs corresponding to two different amplitude peaks in the Fourier spectrum of the original image. As we can see, this filtering process appears to be very efficient for vine plot segmentation, provided that it is followed by a thresholding step and a binary object enumeration.

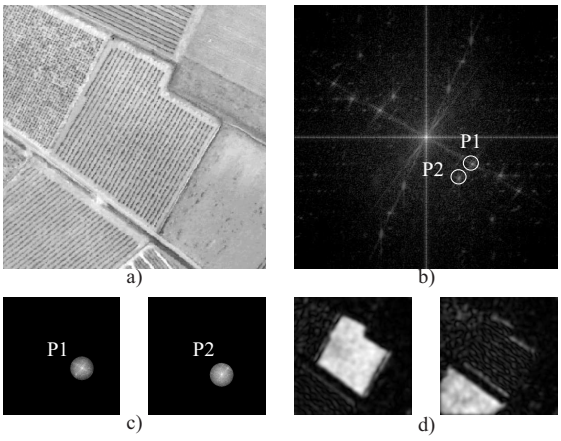

Figure 4: Gabor filtering. a) Original image b) its Fourier transform c) Peak selection using Gabor filters d) modulus of the output complex image for both peaks.

4 ALGORITHM

4.1 Pre-processing

To increase algorithm robustness, an initial normalization step is designed, ensuring that any original image will have approximately the same amplitude of luminance variation from row to inter-row in the vineyard areas. Each pixel value is divided by the local 'textural contrast' around it, defined from Haralick's contrast feature (Haralick et al., 1973). If this one is too low, the corresponding pixel is set to null.

The Gabor filtering process described above must be applied on limited size images (typically 500×500 pixels) both for computational reasons and to get exploitable Fourier spectra. When dealing with large aerial images (typically 5000×5000 pixels), an image partitioning is used. As a result, a set of adjacent sub-images is obtained which will be processed successively. In the following, we only consider such sub-images, and will see how to recover plots that have been split by the partitioning process. Moreover, as the Hanning window tends to decrease image contrast near its edges, adjacent sub-images issued from the initial partitioning step must present a significant overlap to ensure that every portion of the original image is examined under its optimal contrast.

4.2 Filtering process

Gabor filter is applied successively on the various main amplitude peaks in the Fourier spectrum. Thanks to the original image normalization, and to the filter selectivity, a very simple binary thresholding can be applied to the filtered output image, the choice of the threshold value being not critical. Thus, we obtain a binary image, in which every object is supposed to be a vine plot with the same characteristics of orientation and interrow width (given by the current Gabor filter center). However, when several plots have been found using the same Gabor filter, all of them may not have exactly the same characteristics but very close ones. Some plots may also be incomplete in the current original sub-image, if it has been split by the initial partitioning process.

The following procedure is thus followed:

1. The original image Fourier spectrum is computed, and only the highest peak is searched for within potential frequencies of vineyard (given by minimum and maximum interrow width encountered).

2. A Gabor filter, centered on this peak is processed, followed by Fourier inversion and binary thresholding. For each plot found at this step:

   - a new sub-image is created where all pixels but those of the candidate plot are painted in black, so that only its corresponding amplitude peak will appear in the Fourier spectrum. A new Gabor filtering is then applied around this unique peak and the FFT inversion is carried out on the original image to obtain a possibly more closely matching vine plot
   - if the resulting binary object touches a sub-image edge, a new sub-image is built around it with extended margins, and the whole process is reiterated. By this way, we are guaranteed to recover the complete plot in one or several iterations.

3. when the corresponding plots have been completely recovered, they are listed and erased from the original image by painting them in black.

4. The process is reiterated from 1.

This process is stopped in 2. before listing, when the associated plot area is lower than a predefined value given by user.

4.3 Recursive implementation

From the various steps described above, it appears that the same filtering and binary analysis scheme is applied many times, starting either from the initial sub-images, or from the current plot candidate, by building a new sub-image around it. Moreover, the iteration number is not predictable (the sub-image issued from a current binary object can itself generate an undetermined number of new object apparitions). A recursive implementation is then particularly suited. The basic recursive function, starting from a binary object, includes sub-image building, Gabor setting and filtering, and sub-object analysis, this last one generating new function calls if some sub-objects touch the current sub-image edges. The function terminates when no new sub-object with significant area is detected.

This recursive function is summarized in figure 5. It is initially applied on 'virtual' plots issued from the partitioning (and thus considered as incomplete). In order to avoid multiple detections of the same vine plot, a global list of the already detected plots is maintained all along the process, and used to erase the corresponding zones, if any, in every new sub-image before processing.

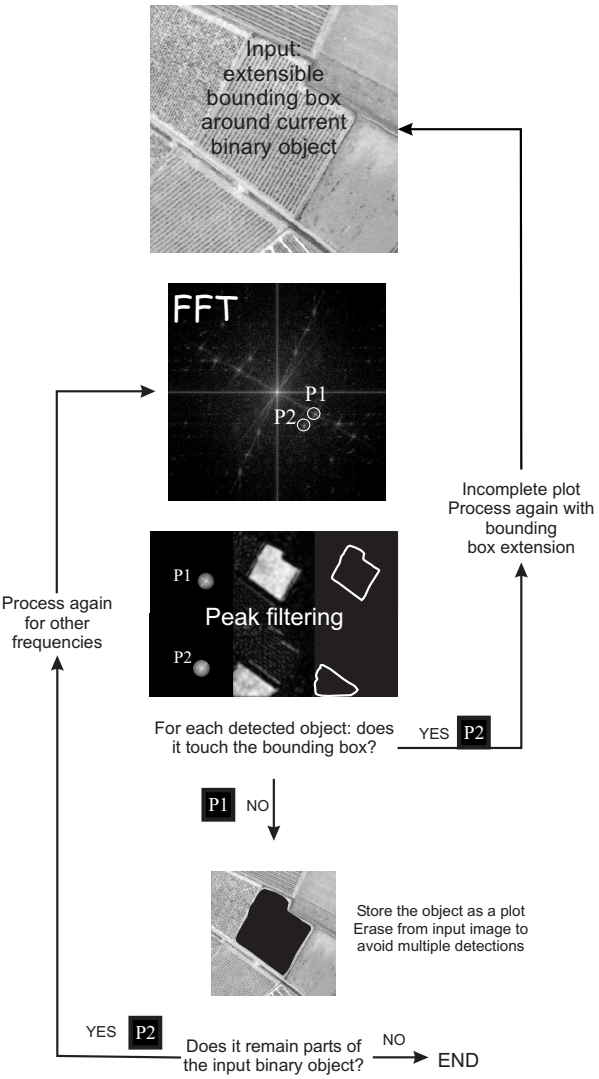

Figure 5: Recursive process applied on each binary object.

5 RESULTS

The main goal of the presented process is the plot contours delineation. Therefore, a plot basis validation has been performed, comparing automatically and manually segmented plots according to their overlapping rate. Eight different cases have been defined (see figure 6):

1. Good segmentation: the overlapping surface of real and automatically segmented plots is higher than 70%.
2. Over-segmentation: several plots are automatically segmented in one real plot.
3. Under-segmentation: one automatically segmented plot includes several real plots.
4. Partial segmentation: only one part of the plot is detected
5. Large segmentation: the automatically segmented plot overflows onto other plots.
6. Missing segmentation: vine plots not automatically segmented
7. Extra segmentation: non-vine plots automatically segmented as vine.
8. Other cases

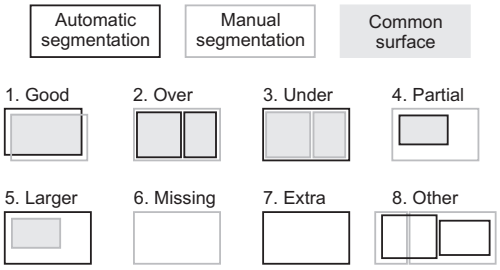

Figure 6: Different cases for segmentation results.

The results obtained according to this classification are given in table 1.

Segmentation type	Real plots (except for 7)	Corresponding surface
1. Good	**41** (36%)	27.5 (36%)
2. Over	1 (0.9%)	2 (2.5%)
3. Under	**24** (21%)	16 (20.8%)
4. Partial	4 (3.5%)	4.2 (5.4%)
5. Larger	3 (2.7%)	1.4 (1.8%)
6. Missing	**40** (35%)	25 (33%)
7. Extra	2 (0.2%)	
8. Other	1 (0.9%)	0.4 (0.5%)
Total (except 7)	114 (100%)	76.5 (100%)

Table 1: Results in number of plots and corresponding surface, according to different segmentation configurations.

Three main types of classification can be considered: well segmented plots (36%), under-segmented plots (21%), and missing plots (35%).

Figure 7, shows some examples of good detection, corresponding to well segmented and under-segmented plots. The latter case typically correspond to the grouping of neighboring plots that have the same row orientation and interrow width, and are only separated by a narrow road or a ditch. Some of them are not spatially separated, and only differ by the soil surface condition between rows (figure 7b) or by some characteristics undistinguishable in aerial images, such as age or height (figure 7c). This kind of segmentation error can nevertheless potentially be managed by further processing, as discussed below.

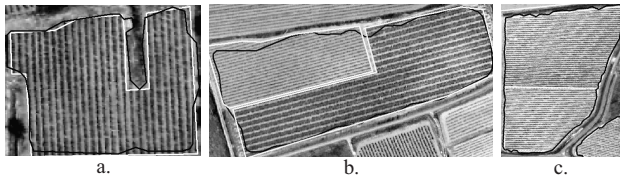

Figure 7: Examples of good detection: (a) Good segmentation; (b) 2 regrouped plots which differ by the soil surface condition between rows; (c) 2 regrouped plots for which difference is nearly undistinguishable on aerial photograph.

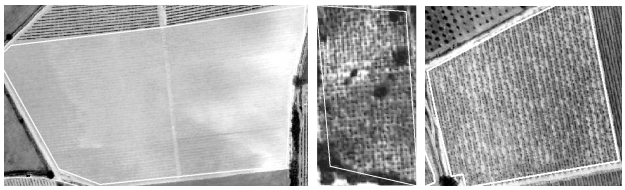

Figure 8: Examples of non-segmented plots: a. young vine whose rows are hardly visible; b. old goblet vine smaller than 0.2ha, with an interrow width of 1.6m; c. vine with a lot of missing vine-trees and a '1 row out of 2' pattern.

A more problematic figure is the ratio of missing plots (35%), though it has, most of the time, an easily comprehensible reason. The first cause of non-segmentation is that the vine is too young (typically less than 3 years old). Vegetation is thus not enough developed for the rows to be visible on aerial photographs (figure 8a). Consequently, only one young vine out of fifteen is correctly segmented, two are under-segmented and all the others are not segmented at all. The second cause of non-segmentation is a small interrow width. This characteristic has a significant consequence concerning the vine training. Indeed, an interrow width lower than about 1.7 m prevents from a mechanized work (owing to the size of tractor or grape harvesting machine). The related vines are thus manually trained and vine-trees are often not pruned in rows, leaving the vegetation growing over interrow. This leads to a low visibility of soil between rows which is worsened by the interrow width itself, closed to detection limit according to image resolution. Moreover, manually trained vines are generally older, smaller and sometimes less maintained (figure 8b). Other missing detection can be due to:

- an alternated treatment between interrows: the main pattern period is then twice or fourth the interrow width, leading to a reduced peak amplitude in the relevant frequency range (figure 8c);
- a high number of missing vine trees (figure 8c);
- a too small size (4 real plots were not detected because their area was lower than the threshold value, 1000 m^2).

Moreover, the ratio of missing detections falls to about 17%, when considering adult vines with reasonable size and interrow width. Indeed, 100% of small vines (less than 1000 m^2) are not

detected, 80% of young vine (less than 3 years old) and 55% of narrow vines (with an interrow width lower than 1.7 m).

Other figures in table 1 mainly concern plots that present heterogeneities due to bad cultivation conditions (poor foliage development, missing trees, etc.). This generally leads to partial segmentation, or larger segmentation if combined with plot grouping: this last case concerns 2.7% of vine plots but only 1.8% of vine cultivated surface, indicating it mainly affects small plots.

6 CONCLUSIONS AND FUTURE WORK

The proposed recursive approach has proved its efficiency for vineyard detection and characterization in many ways. While most of detection studies - not only concerning vineyards - provide a pixel classification, the main originality of this method is that results are directly available in a polygonal form, thanks to the automatic segmentation process. Another significant advantage is that largely available data can be used. Indeed, the method does not requires any multi-spectral information, and can be successfully applied on the red channel of an aerial image. Moreover, since the appropriate spatial resolution is linked to the researched pattern period, a poorer resolution could be used in many other vine-growing regions, especially dry regions such as in Spain where interrow widths are up to 3 m. Then, satellite images, such as those provided by Ikonos or Quickbird, could be used.

Using frequency analysis, very precise information of row orientation and interrow width can be deduced from the peak position in the Fourier spectrum. Accuracy of these characteristics depends on the quantity of information in the original image, *i.e.* on the number of rows in the vine plot, but is generally very good.

In terms of performance, the present study has nevertheless shown some limitations, especially concerning under-segmented plots and missing detections. The case of under-segmentation, which consists in grouping neighboring plots with very similar characteristics, can be considered as a side effect of a generally poor accuracy in plot edge definition. This poor accuracy is inherent to any segmentation method, including this one, relying on textural pattern detection: a minimal neighborhood is required to detect such patterns, leading to a limited spatial resolution of the segmentation. For this reason, we do believe that a further step based on individual vine row analysis is necessary (and probably sufficient) to overcome this type of problems. It is presently under development. In addition to the utility of characterization as such, accurate estimations of interrow width and row orientation as given by the present method are thus very useful in such a further step requiring individual row detection.

The cases of missing detection are more problematic, in the sense that no further improvement step can be envisaged. As seen above, they concern very poorly visible vine plots (mainly young or badly maintained ones) and therefore show a limitation of aerial imaging approach itself.

Finally, another limit of this method is that it has to be applied on linear row patterns; important modifications would be needed to apply such a method on level line vineyards such as there are in Portugal.

ACKNOWLEDGEMENTS

The present study has been partly carried out within the European research project Bacchus (www.bacchus-project.com) with a cofunding from the European Commission.

REFERENCES

Barbezat, V., Kreiss, P., Sulzmann, A. and Jacot, J., 1996. Automated recognition of forest patterns using aerial photographs. In: SPIE: Optics in Agriculture, Forestry, and Biological Processing II, Bellingham (Washington).

Bobillet, W., Da Costa, J.-P., Germain, C., Lavialle, O. and Grenier, G., 2003. Row detection in high resolution remote sensing images of vine fields. In: J. Stafford and A. Werner (eds), European Conference on Precision Agriculture, Wageningen academic publishers, Berlin, pp. 81–87.

Chanussot, J., Bas, P. and Bombrum, L., 2005. Airborne remote sensing of vineyards for the detection of dead vine trees. In: Geoscience and Remote Sensing Symposium, IGARSS '05, Seoul Corea (IEEE International), Vol. 5, pp. 3090– 3093.

Franklin, S. E., Hall, R. J., Moskal, L. M., Maudie, A. J. and Lavigne, M. B., 2000. Incorporating texture into classification of forest species composition from airborne multispectral images. International Journal of Remote Sensing 21, pp. 61–79.

Gabor, D., 1946. Therory of communication. Journal of the Institution of Electrical Engineers 93(26), pp. 429–457.

Garcin, L., Descombes, X., J., Z. and H., L. M., 2001. Building detection by markov object processes and a mcmc algorithm. Technical Report 4206, INRIA.

Hall, A., Louis, J. and Lamb, D., 2003. Characterising and mapping vineyard canopy using high-spatial-resolution aerial multispectral images. Computers and Geosciences 29, pp. 813–822.

Haralick, R., Shanmugam, K. and Dinstein, I., 1973. Textural features for image classification. IEEE Transaction on Systems, Man, and Cybernetics 3, pp. 610–621.

Jain, A. K. and Farrokhnia, F., 1991. Unsupervised texture segmentation using gabor filters. Pattern Recognition 24, pp. 1167–1186.

Moskal, L., 2002. Investigating texture inversion in high-resolution multispectral imagery; implications for forest classification. In: Annual conference and FIG XXII Congress, Washington, D. C.

Ranchin, T., Naert, B., Albuisson, M., Boyer, G. and Astrand, P., 2001. An automatic method for vine detection in airborne imagery using wavelet transform and multiresolution analysis. Photogrammetric Engineering and Remote Sensing 67(1), pp. 91–98.

Segl, K., Roessner, S., Heiden, U. and Kaufmann, H., 2003. Fusion of spectral and shape features for identification of urban surface cover types using reflective and thermal hyperspectral data. ISPRS Journal of Photogrammetry and Remote Sensing 58, pp. 99–112.

Wassenaar, T., Andrieux, P., Baret, F. and Robbez-Masson, J., 2005. Soil surface infiltration capacity classification based on the bi-directional reflectance distribution function sampled by aerial photographs. the case of vineyards in a mediterranean area. Catena 62, pp. 94–110.

Wassenaar, T., Robbez-Masson, J.-M., Andrieux, P. and Baret, F., 2002. Vineyard identification and description of spatial crop structure by per-field frequency analysis. International Journal of Remote Sensing 23(17), pp. 3311–3325.

Weldon, T. P., Higgins, W. E. and Dunn, D. F., 1996. Efficient gabor filter design for texture segmentation. Pattern Recognition 29, pp. 2005–2015.